

Prophylactic treatment with sialic acid metabolites precludes the development of the myopathic phenotype in the DMRV-hIBM mouse model

May Christine V Malicdan^{1,2}, Satoru Noguchi¹, Yukiko K Hayashi¹, Ikuya Nonaka¹ & Ichizo Nishino¹

Distal myopathy with rimmed vacuoles (DMRV)–hereditary inclusion body myopathy (hIBM) is an adult-onset, moderately progressive autosomal recessive myopathy; eventually, affected individuals become wheelchair bound¹. It is characterized clinically by skeletal muscle atrophy and weakness, and pathologically by rimmed vacuoles, which are actually accumulations of autophagic vacuoles^{2–4}, scattered angular fibers and intracellular accumulation of amyloid and other proteins⁵. To date, no therapy is available for this debilitating myopathy, primarily because the disease pathomechanism has been enigmatic. It is known that the disease gene underlying DMRV-hIBM is *GNE*, encoding glucosamine (UDP-*N*-acetyl)-2-epimerase and *N*-acetylmannosamine kinase^{6–8}—two essential enzymes in sialic acid biosynthesis⁹. It is still unclear, however, whether decreased sialic acid production causes muscle degeneration, as *GNE* has been proposed to have roles other than for sialic acid biosynthesis^{10–12}. By showing that muscle atrophy and weakness are completely prevented in a mouse model of DMRV-hIBM after treatment with sialic acid metabolites orally, we provide evidence that hyposialylation is indeed one of the key factors in the pathomechanism of DMRV-hIBM. These results support the notion that DMRV-hIBM can potentially be treated simply by giving sialic acids, a strategy that could be applied in clinical trials in the near future.

Sialic acids are the most abundant terminal monosaccharides on glycoconjugates of eukaryotic cell surfaces and are involved in a variety of cellular functions⁹. As *GNE* enzymatic activity measured *in vitro* in cells transfected with mutated *GNE* constructs is reduced by 70–90%¹³, hyposialylation is thought to contribute to the pathogenesis of DMRV-hIBM^{8,13,14}. The role of hyposialylation is further supported by the phenotype of the DMRV-hIBM mouse model, in which *Gne*-deficient mice transgenically express the human *GNE* gene with D176V mutation (*Gne*^{-/-}hGNED176V-Tg)¹⁵. These mice show hyposialylation in various organs in addition to the characteristic features of muscle atrophy, weakness and degeneration and amyloid deposition. In these mice, hyposialylation is documented from birth¹⁵, yet they only develop muscle symptoms several weeks later, including

decreased twitch force production in isolated muscles starting at 10 weeks of age and impairment of motor performance from 20 weeks of age onward¹⁶.

Addition of sialic acid metabolites has been shown to recover overall sialylation in cells^{9,13}. The challenge in administering sialic acid *in vivo*, however, is mainly its rapid excretion in the urine. After a single intraperitoneal injection of *N*-acetylneuraminic acid (NeuAc), the most abundant sialic acid, the sialic acid concentration in the serum is considerably increased within minutes (Supplementary Fig. 1a,c online); but 90% of the sialic acid is found in the urine within 5–30 min, and almost all of it is excreted within 4 h (Supplementary Fig. 1b,d). After a single dose of NeuAc by the intragastric route, the sialic acid concentration in the serum is half that achieved by the intraperitoneal route, but the excretion rate is slower, as 70% of the sialic acid is found in the urine within 30–60 min (Supplementary Fig. 1b,d). We observed a similar pattern of excretion after a single dose of the physiological sialic acid precursor, *N*-acetylmannosamine (ManNAc)¹⁷ (Supplementary Fig. 1e,f). These results suggest that NeuAc and ManNAc are rapidly excreted, and that the intragastric route may be more advantageous in increasing the serum abundance of sialic acid.

As ManNAc is converted to NeuAc after delivery into cells¹⁸, it is potentially a rich source of sialic acid *in vivo*. In the initial portion of this study, we evaluated the efficacy of ManNAc as a treatment for disease in four groups of DMRV-hIBM mice aged 5–6 weeks. At this age, the mice already have hyposialylation, but without obvious signs of myopathy¹⁵. The DMRV-hIBM mice received either water (control treatment; $n = 5$) or ManNAc in their drinking water with an increasing dosing schedule (computed as mg per kg bodyweight per day): the low dose was 20 mg ($n = 5$), the medium dose was 200 mg ($n = 4$) and the high dose was 2,000 mg¹⁹ ($n = 4$). Equal numbers of unaffected littermates (whose genotypes are *Gne*^{+/-} or *Gne*^{+/-}hGNED176V-Tg; we have previously shown that these mice do not have any symptoms¹⁵) for each group were also treated ($n = 18$). We treated mice continuously until 54–57 weeks of age and found an improvement in the survival of DMRV-hIBM mice, as compared to control treatment, in all treatment groups (Fig. 1a), with a statistical trend favoring the medium- and high-dose groups, which both

¹Department of Neuromuscular Research, National Institute of Neuroscience, National Center of Neurology and Psychiatry, Tokyo, Japan. ²Department of Neurology, Kyoto University Graduate School of Medicine, Kyoto, Japan. Correspondence should be addressed to S.N. (noguchi@ncnp.go.jp).

Received 29 December 2008; accepted 6 April 2009; published online 17 May 2009; doi:10.1038/nm.1956

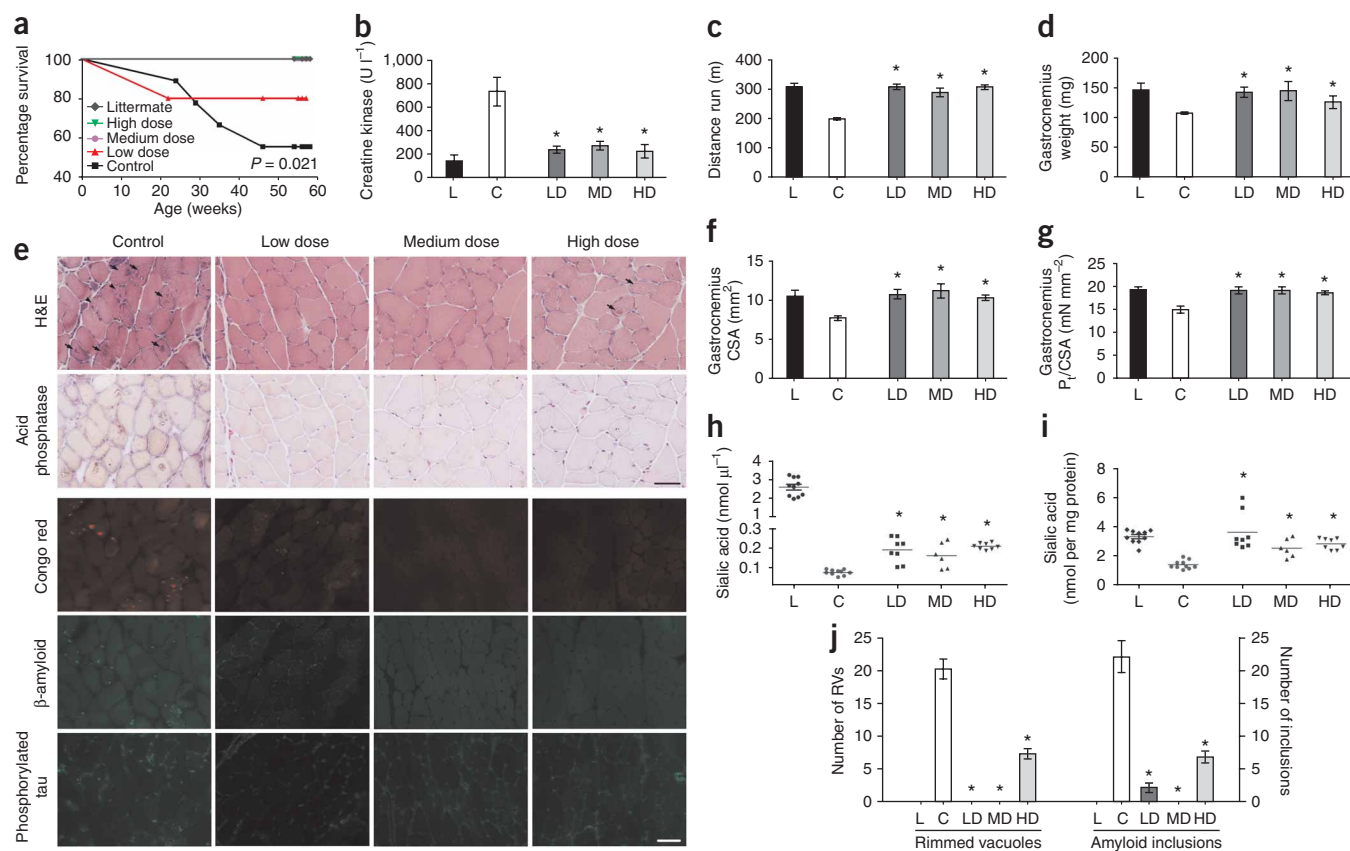


Figure 1 Favorable effects in the myopathic phenotype of DRMV-hIBM mice are seen after administration of ManNAc but are not correlated with dose. (a) Survival rate of DRMV-hIBM mice after treatment with a low dose, medium dose or high dose of ManNAc ($P < 0.05$) as compared to control treatment. (b) Serum creatine kinase concentrations of DRMV-hIBM mice after treatment with all doses of ManNAc. Values for littermates (L) are shown for comparison. C, control treatment; LD, low dose; MD, medium dose; HD, high dose. $*P < 0.05$. (c) Treadmill motor performance in the three ManNAc-treated groups. (d) Gastrocnemius weight after treatment with ManNAc. (e) H&E, acid phosphatase, Congo red, β -amyloid and phosphorylated tau staining of muscle cryosections. Arrows point to rimmed vacuoles; arrowheads point to areas of atrophy. Scale bar, 50 μ m. (f) Physiological CSA of the gastrocnemius after ManNAc treatment. $*P < 0.05$. (g) Production of specific isometric force (P_i /CSA) after ManNAc treatment. $*P < 0.05$. (h) Serum sialic acid concentration after ManNAc treatment. $*P < 0.05$. (i) Membrane-bound sialic acid abundance after treatment with all ManNAc doses. $*P < 0.05$. (j) Number of rimmed vacuoles (RVs) and amyloid inclusions in whole gastrocnemius section. $*P < 0.05$.

displayed 100% survival, over the low-dose group, which showed only a partial improvement in survival. Treatment lowered the serum creatine kinase concentration (Fig. 1b) and led to an increase in parameters assessing overall motor performance, including treadmill performance and endurance tests and a hanging test (Fig. 1c and Supplementary Fig. 2a,b online). Likewise, treatment with ManNAc also increased body weight (Supplementary Fig. 2c) and muscle mass (Fig. 1d) and led to a marked change in pathology (Fig. 1e). Only one among the treated mice had rimmed vacuoles, and the number of rimmed vacuoles was significantly lower than that among mice who received control treatment ($*P < 0.05$). Treatment also increased muscle cross-sectional area (CSA) (Fig. 1f) and force production (Fig. 1g and Supplementary Fig. 3a–d online) and substantially diminished congophilic, amyloid-positive and tau-positive inclusions (Fig. 1e). One treated mouse in the low-dose group and one in the high-dose group showed intracellular amyloid deposits (data not shown). Of note, the number of deposits in these mice was notably lower than in control-treated mice. We did not observe expression of LC3 and Lamp2, which are markers for autophagosomal structures, in the muscle sections of treated mice, except for one mouse that had few rimmed vacuoles in the muscle (Supplementary Fig. 4 online). The favorable results in skeletal muscle parameter measurements were

accompanied by an increase in sialic acid in the serum (Fig. 1h) and an increase in membrane-bound sialic acid in muscle (Fig. 1i) and other organs (Supplementary Fig. 5a online). In addition to the considerable change in pathology, the number of rimmed vacuoles and intracellular amyloid inclusions was markedly reduced (Fig. 1j). For all parameters tested, we did not observe dose dependence.

ManNAc was tolerated well by the treated mice, as kidney and liver function tests were normal (Supplementary Table 1 online). In the high-dose group, however, both of the female DRMV-hIBM mice in the group showed multiple ovarian masses after treatment (data not shown), suggesting a possible caveat in using high doses of ManNAc. Histopathological findings in these ovarian masses were akin to those of polycystic ovarian cysts, containing both hemorrhagic and fluid-filled cysts, in addition to hyperemia; on careful examination, we did not find any signs of malignancy (data not shown).

Because the 20-mg dose of ManNAc was effective in preventing the myopathic symptoms in majority of the DRMV-hIBM mice, we subsequently used this low dose in another cohort of mice to evaluate the efficacy of other metabolites. We gave four groups of 10- to 20-week-old DRMV-hIBM mice either ManNAc ($n = 6$), NeuAc ($n = 5$), sialic acid conjugate (sialyllactose, $n = 7$) or water (as control treatment; $n = 10$) continuously until 54–57 weeks of age. We

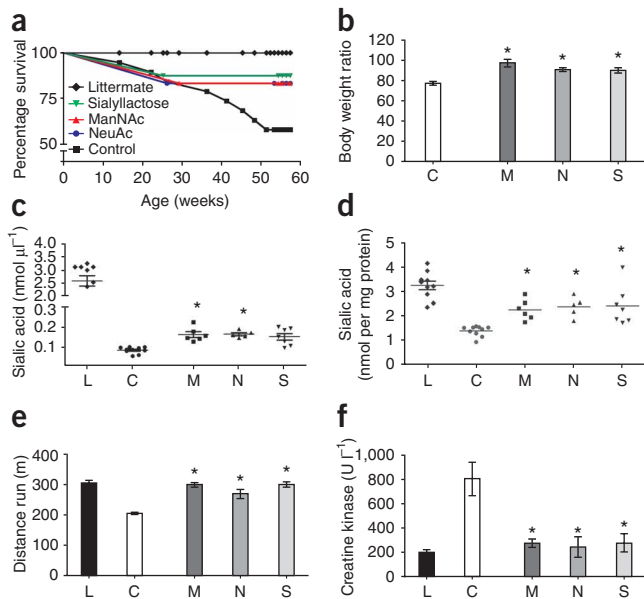


Figure 2 Low-dose administration of ManNAc, NeuAc or sialyllactose increases the sialic acid concentration in serum and muscle and leads to an improvement in survival and favorable effects on overall motor performance. **(a)** Survival curve of treated DMRV/hIBM mice after treatment with ManNAc ($P < 0.05$), NeuAc ($P < 0.05$), sialyllactose ($P < 0.05$) as compared to control treatment. **(b)** Body weight ratio of DMRV-hIBM mice treated with NeuAc ($P < 0.05$), sialyllactose ($P < 0.05$) and ManNAc ($P < 0.01$). C, control treatment; M, ManNAc; N, NeuAc; S, sialyllactose. **(c)** Serum sialic acid concentration after treatment either with ManNAc, NeuAc or sialyllactose as compared with control treatment. L, littermate. **(d)** Bound sialic acid in the muscle after treatment with sialic acid ($P < 0.05$ for all treated groups) as compared with control treatment. **(e)** Treadmill performance test evaluating the distance mice could run. **(f)** Serum creatine kinase concentration in treated mice as compared to those in control treatment. For all parameters tested, there is no statistical difference among the three agents used in the study.

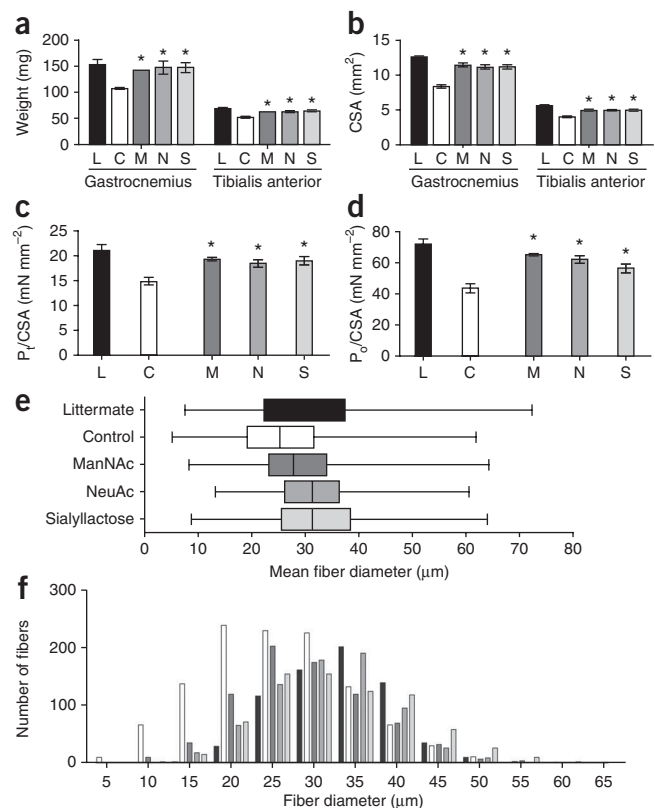
amounts of the bound forms of sialic acids in the three treatment groups as compared to the control-treated group.

Treated DMRV-hIBM mice performed better than control-treated mice in running on a treadmill (Fig. 2e), enduring a specific running workload (Supplementary Fig. 6a online) and holding on to an inverted mesh wire (Supplementary Fig. 6b). Overall, the motor performance of the treated DMRV-hIBM mice almost reached that achieved by nondiseased littermates and was paralleled by a decrease in serum creatine kinase values (Fig. 2f). Previously, we showed that muscle weakness or decreased production of force is largely due to atrophy during the early stages of the disease and is compounded at the later stages by rimmed vacuole formation and muscle degeneration²¹. In the current study, treated mice showed an increase in weight (Fig. 3a) and CSAs of gastrocnemius and tibialis anterior muscles (Fig. 3b). Furthermore, *ex vivo* measurement of force in isolated muscles showed a marked increase in both the specific isometric

also treated equal numbers of littermate controls for each group ($n = 18$). At 10–20 weeks of age, the DMRV-hIBM mice show only early reduction in production of force (detected by *ex vivo* analysis of muscle contractile properties), but no apparent muscle weakness, in addition to hyposialylation of most organs¹⁶. Thus, in this study, this treatment protocol is designed for the prevention of disease. Sialyllactose is a conjugated sialic acid that contains about 45% sialic acid. It is the major source of sialic acid in milk in addition to κ -casein²⁰. All agents were well tolerated at a dose of 20 mg per kg body weight per day (Supplementary Table 1). Treatment with any of the three sialic acid compounds improved the survival of the DMRV-hIBM mice versus the control-treated group, from a median survival at 54–57 weeks of 55.6% to one of 86.9%, and reduced the hazard ratio from 34.05 to 0.26 (Fig. 2a). Also, with treatment the body weight of treated DMRV-hIBM mice increased as compared to the control-treated group (Fig. 2b).

We next addressed the relationship between hyposialylation and the development of myopathic symptoms in DMRV-hIBM mice. After treatment, there was a modest increase in the serum sialic acid, but it was only significant in ManNAc-treated ($P = 0.038$) and NeuAc-treated ($P = 0.001$) groups (Fig. 2c). In muscle (Fig. 2d) and other organs (Supplementary Fig. 5b), there were considerably larger

Figure 3 Oral administration of sialic acid metabolites notably prevents atrophy in skeletal muscles and increases generation of force. **(a)** Weight of the isolated gastrocnemius and tibialis anterior muscles in DMRV-hIBM mice after treatment with ManNAc (M), NeuAc (N) or sialyllactose (S) as compared to control treatment (C) and littermate (L). **(b)** Whole-muscle CSA of both gastrocnemius and tibialis muscles in the DMRV-hIBM mice after treatment either with ManNAc, NeuAc or sialyllactose. **(c,d)** Contractile properties of the gastrocnemius muscle, as determined by *ex vivo* measurement of specific isometric force (P_0 /CSA) **(c)** and specific tetanic force (P_0 /CSA) **(d)**. For **a–d**, $*P < 0.05$ for ManNAc-treated, NeuAc-treated and sialyllactose-treated mice as compared to control-treated mice. For all parameters tested, there is no statistical difference among the three agents used in the study. **(e)** Mean diameter of individual fibers in the gastrocnemius after treatment with either ManNAc, NeuAc or sialyllactose ($*P < 0.05$). A total of 1,000–1,500 fibers were counted. **(f)** Histogram of individual muscle fiber diameters. The histogram is shifted to the left as the numbers of atrophic fibers in the DMRV/hIBM mice after treatment either with ManNAc, NeuAc or sialyllactose are reduced.



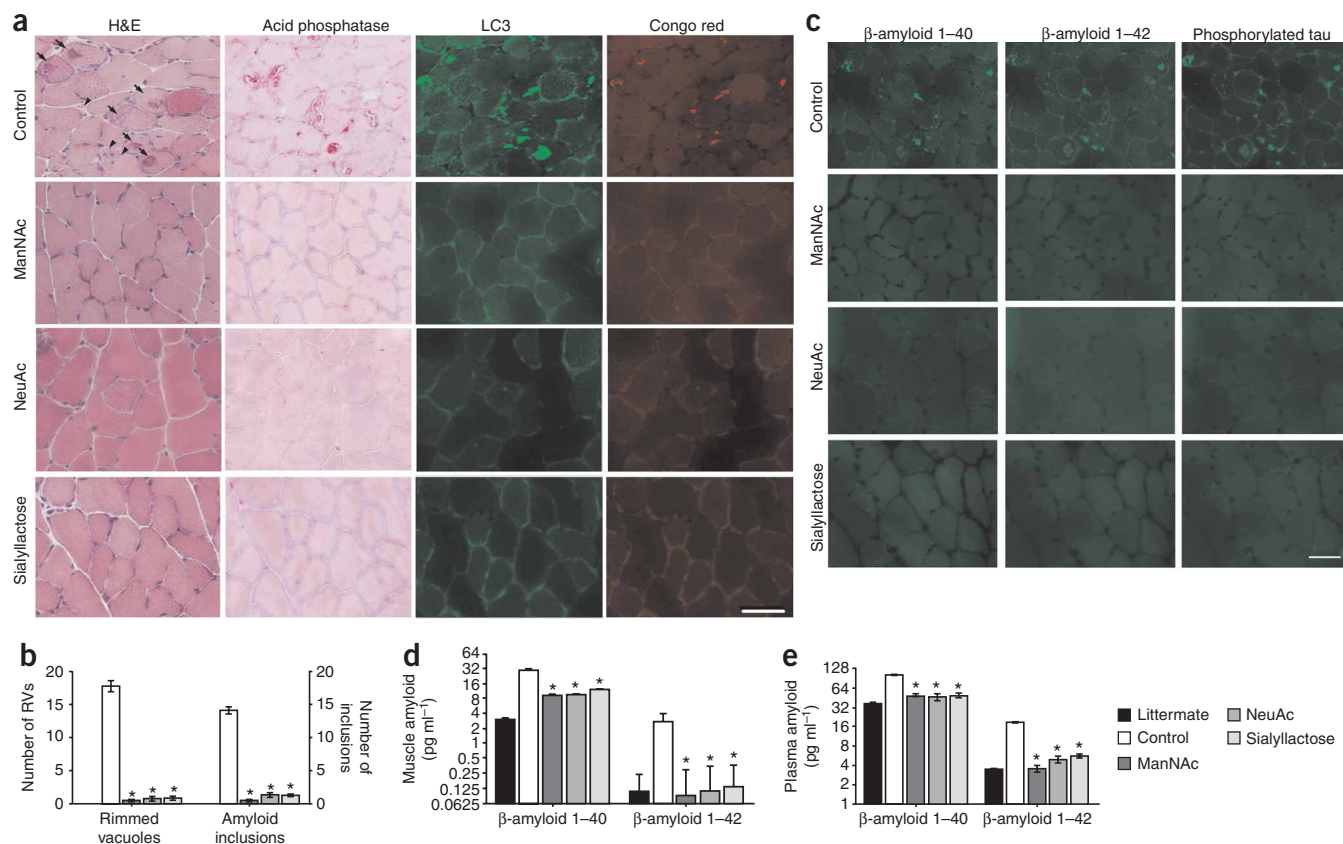


Figure 4 Muscle degeneration in DMRV-hIBM mice is virtually abrogated after oral treatment with sialic acid metabolites. **(a)** H&E staining of gastrocnemius sections: rimmed vacuoles (arrows) and atrophic fibers (arrowheads) are shown in cryosections of control DMRV-hIBM mice. Scale bar, 50 μ m. **(b)** Number of rimmed vacuoles and amyloid inclusions in a whole section of gastrocnemius after sialic acid treatment ($P < 0.05$ for ManNAc, NeuAc and sialyllactose). **(c)** Intracellular deposition β -amyloid and phosphorylated. Scale bar, 50 μ m. **(d)** β -amyloid 1–40 and 1–42 in muscle by ELISA ($*P < 0.05$ for ManNAc, NeuAc and sialyllactose). **(e)** Plasma amyloid abundance as detected by ELISA. $P < 0.05$ for ManNAc, NeuAc and sialyllactose as compared to control treatment. The key applies to **b**, **d** and **e**.

(Fig. 3c) and specific tetanic (Fig. 3d) forces in the gastrocnemius and tibialis anterior muscles (see **Supplementary Fig. 7a,b** online) after treatment. Notably, although the twitch-tetanic ratio was increased in the gastrocnemius in older DMRV-hIBM mice¹⁶, it was significantly reduced only in NeuAc-treated ($P < 0.05$) and ManNAc-treated ($P < 0.05$) groups (**Supplementary Fig. 7c**).

The increase in force generation was proportional to the increase in muscle area but not to the number of fibers, suggesting that the increase in force production is probably due to an increase in single-fiber diameter, and this is exemplified by the smaller number of atrophic fibers in the gastrocnemius muscles of the three treatment groups (Fig. 3e,f) when compared to control-treated mice. As we have previously implied¹⁶, atrophy in DMRV-hIBM mice seems to follow a mechanism distinct from the canonical pathways of atrophy in the muscle²¹. In DMRV-hIBM mice, because atrophy is prevented by increasing muscle sialylation, a causal relationship between hyposialylation and atrophic cascade is suggested.

Rimmed vacuoles and intracellular deposits presumably contribute to the loss of muscle power in DMRV-hIBM mice, especially as they age¹⁶. Rimmed vacuoles are most likely activated secondarily to cellular events such as protein misfolding or aggregation. Although all mice in the control-treated group showed rimmed vacuoles in the gastrocnemius, only a few in the treatment groups showed rimmed vacuoles (Fig. 4a). In DMRV-hIBM mice, the chance of developing rimmed vacuoles was substantially lower after treatment with

ManNAc (odds ratio, 1.8%), NeuAc (odds ratio, 2.2%) and sialyllactose (odds ratio, 1.3%) as compared to control treatment (100%). Likewise, in those treated mice that had rimmed vacuoles, the number of rimmed vacuoles was much smaller than in control-treated mice (Fig. 4b). As rimmed vacuoles are autophagic in nature^{2–4}, we checked for acid phosphatase staining and immunoreactivity to LC3 and Lamp2 and found decreased staining for these proteins (Fig. 4a). The amounts of LC3-I and LC3-II, used as an index to analyze autophagic induction in tissues^{22,23}, were lower in the skeletal muscles after treatment (**Supplementary Fig. 8** online).

In DMRV-hIBM mice, intracellular amyloid inclusions in muscles have been noted to occur earlier than rimmed vacuole formation¹⁵. We examined skeletal muscle cryosections and found out that only a few mice in the treatment groups showed such accumulations (Fig. 4a–c), with the percentage of metabolite-treated mice having such inclusions being substantially lower than for the control-treated group. The chance of having amyloid accumulations is likewise lower in the treatment group: 1.3% for ManNAc, 1.6% for NeuAc and 0.9% for sialyllactose. To quantify the amount of amyloid burden in the muscle and plasma, we measured the amount of β -amyloid peptides 1–40 and 1–42, both of which accumulate in the muscles of DMRV-hIBM mice¹⁵, by ELISA in total muscle homogenate (Fig. 4d) and plasma (Fig. 4e) and found their expression noticeably decreased after treatment with ManNAc, NeuAc and sialyllactose. Treatment lowered both amyloid 1–40 and 1–42 abundance with

the same efficacy. Likewise, the amount of the C99 fragment of β -amyloid precursor protein was also decreased after treatment (Supplementary Fig. 9 online).

We also evaluated various proteins, such as phosphorylated tau⁵ and polyubiquitinated proteins²⁴, which are known to accumulate in muscles of DMRV-hIBM mice, and did not find immunoreactive signals for phosphorylated tau (Fig. 4e) or polyubiquitinated proteins (data not shown) after treatment.

Here we have shown that hyposialylation is one of the key factors in the pathomechanism of DMRV-hIBM. We have also provided evidence that prophylactic treatment with ManNAc, using three different doses, prevented the myopathic phenotype in the majority of the DMRV-hIBM mice and substantially reduced the number of rimmed vacuoles and amyloid accumulations in a few DMRV-hIBM mice. We did not observe dose-dependent efficacy when we compared all parameters, although the survival rate was better for the medium- and high-dose groups, and serum sialic acid was higher among those who received the high dose (Fig. 1e,i,j). There is no straightforward explanation as to why we do not see a clear dose-dependent efficacy of ManNAc treatment in DMRV-hIBM mice. Taking the pharmacokinetic properties of NeuAc and ManNAc into consideration, it can be surmised that even if one gives a higher dose, not all of the metabolite administered through the oral route is delivered into the muscle. Alternatively, one may hypothesize that the muscle has some maximum limit for actually incorporating sialic acid, such that increasing the oral dose of metabolite would not be translated into increasing the sialic acid pool in muscle. However, more experiments are needed to clarify this issue, including the use of labeled sialic acid and tracing the amount incorporated (distribution) into the tissue to compare the different doses *in vivo*. The absence of a clear dose response is difficult to explain but may also imply a need for more sensitive methods in analyzing the molecular markers in DMRV-hIBM.

Our results suggest that increasing the sialylation status, at least in muscle, can prevent the development of the myopathic phenotype in the majority of treated DMRV-hIBM mice or at least delay the progression in the few DMRV-hIBM mice that eventually show some rimmed vacuoles in skeletal muscle, despite a marked improvement in muscle performance. The increase in sialic acid abundance in the muscle and various organs after oral administration of sialic acid metabolites is consistent with the increase in protein sialylation after ManNAc administration in the recently used mouse knock-in model of the *GNE* M712T mutation, in which the mice developed podocytopathy¹⁹. Although the role of amyloid deposition within the myofibers has not been clarified, it should be noted that sialic acid has some role in conferring stability on glycoproteins^{25,26} and might act as scavenger of radicals such as H₂O₂ (ref. 27), both of which roles have been implicated in amyloidogenesis and hence could be affected when total sialic acid abundance is decreased in muscle. From our data, it can be surmised that correction of hyposialylation might reduce the amyloid burden in muscles. Nevertheless, this intracellular β -amyloid accumulation may be an epiphenomenon to hyposialylation, as amyloid deposition has been noted in a variety of myopathies^{28,29}. Recently, it has been demonstrated that neprilysin, a metalloproteinase β -amyloid precursor protein-processing enzyme, is hyposialylated and has reduced expression and enzymatic activity in hIBM muscles; this implies that hyposialylation might impair neprilysin and contribute to increased accumulation of β -amyloid peptides.

In conclusion, our results support the concept that hyposialylation in this myopathy should not be considered merely as a by-product of a

metabolic impairment, but rather as one of the factors behind the pathomechanism of the disease. There are still several issues that need to be addressed, such as the absence of clear dose response efficacy to ManNAc and the role of sialic acid itself in muscle metabolism, and, more importantly, the therapeutic effect of sialic acid metabolites in DMRV-hIBM. Nevertheless, from our data we can conclude that replenishment of the total sialic acid in muscle by administering sialic acid precursor, sialic acid itself or sialic acid conjugate considerably prevents skeletal muscle atrophy, loss of power and myofiber degeneration in the DMRV-hIBM mouse model. More notably, our data corroborate the concept that DMRV-hIBM is a potentially treatable myopathy. Low-dose NeuAc, ManNAc and sialyllactose are effective in improving the sialylation status in the muscle and serum and may be considered in future clinical trials.

METHODS

Methods and any associated references are available in the online version of the paper at <http://www.nature.com/naturemedicine/>.

Note: Supplementary information is available on the Nature Medicine website.

ACKNOWLEDGMENTS

The authors acknowledge the valuable assistance offered by F. Funato and R. Hoshi in motor performance evaluation of mice, toxicology assays and sialic acid measurement. This study is supported partly by the Research on Psychiatric and Neurological Diseases and Mental Health grant from the Japanese Health Sciences Foundation; the Program for Promotion of Fundamental Studies in Health Sciences of the Japanese National Institute of Biomedical Innovation the Research Grant (19A-7) for Nervous and Mental Disorders from the Ministry of Health Labour and Welfare in Japan, the Kato Memorial Trust for Nambu Research and the Neuromuscular Disease Foundation.

AUTHOR CONTRIBUTIONS

M.C.V.M. conducted most of the experiments and wrote the manuscript; S.N. supervised all aspects of this study, including study design, execution and interpretation and manuscript preparation, and participated in the analysis of the *in vitro* muscle data and sialic acid measurement; I. Nonaka, Y.K.H. and I. Nishino were involved in analyzing and interpreting all the data and also supervised the study design, execution and interpretation and manuscript preparation.

COMPETING INTERESTS STATEMENT

The authors declare competing financial interests: details accompany the full-text HTML version of the paper at <http://www.nature.com/naturemedicine/>.

Published online at <http://www.nature.com/naturemedicine/>

Reprints and permissions information is available online at <http://npg.nature.com/reprintsandpermissions/>

1. Nonaka, I., Noguchi, S. & Nishino, I. Distal myopathy with rimmed vacuoles and hereditary inclusion body myopathy. *Curr. Neurol. Neurosci. Rep.* **5**, 61–65 (2005).
2. Nishino, I. *et al.* Molecular pathomechanism of distal myopathy with rimmed vacuoles. *Acta Myol.* **24**, 80–83 (2005).
3. Tsuruta, Y. *et al.* Expression of the lysosome-associated membrane proteins in myopathies with rimmed vacuoles. *Acta Neuropathol.* **101**, 579–584 (2001).
4. Malicdan, M.C., Noguchi, S. & Nishino, I. Autophagy in a mouse model of distal myopathy with rimmed vacuoles or hereditary inclusion body myopathy. *Autophagy* **3**, 396–398 (2007).
5. Askanas, V. & Engel, W.K. Hereditary inclusion myopathies. in *The molecular and genetic basis of neurologic and psychiatric disease* (eds. Rosenberg, R.N., Prusiner, S.B., DiMauro, S., Barchi, R.L. & Nestler, E.J.) 501–509 (Butterworth-Heinemann, Woburn, Massachusetts, 2003).
6. Eisenberg, I. *et al.* The UDP-*N*-acetylglucosamine 2-epimerase/*N*-acetylmannosamine kinase gene is mutated in recessive hereditary inclusion body myopathy. *Nat. Genet.* **29**, 83–87 (2001).
7. Ikeuchi, T. *et al.* Gene locus for autosomal recessive distal myopathy with rimmed vacuoles maps to chromosome 9. *Ann. Neurol.* **41**, 432–437 (1997).
8. Nishino, I. *et al.* Distal myopathy with rimmed vacuoles is allelic to hereditary inclusion body myopathy. *Neurology* **59**, 1689–1693 (2002).
9. Keppler, O.T. *et al.* UDP-GlcNAc 2-epimerase: a regulator of cell surface sialylation. *Science* **284**, 1372–1376 (1999).

10. Krause, S. *et al.* Localization of UDP-GlcNAc 2-epimerase/ManAc kinase (GNE) in the Golgi complex and the nucleus of mammalian cells. *Exp. Cell Res.* **304**, 365–379 (2005).
11. Wang, Z., Sun, Z., Li, A.V. & Yarema, K.J. Roles for GNE outside of sialic acid biosynthesis: modulation of sialyltransferase and BiP expression, GM3 and GD3 biosynthesis, proliferation and apoptosis, and ERK1/2 phosphorylation. *J. Biol. Chem.* **281**, 27016–27028 (2006).
12. Amsili, S. *et al.* UDP-N-acetylglucosamine 2-epimerase/N-acetylmannosamine kinase (GNE) binds to α -actinin 1: novel pathways in skeletal muscle? *PLoS One* **3**, e2477 (2008).
13. Noguchi, S. *et al.* Reduction of UDP-N-acetylglucosamine 2-epimerase/N-acetylmannosamine kinase activity and sialylation in distal myopathy with rimmed vacuoles. *J. Biol. Chem.* **279**, 11402–11407 (2004).
14. Broccolini, A. *et al.* Hyposialylation of neprilysin possibly affects its expression and enzymatic activity in hereditary inclusion-body myopathy muscle. *J. Neurochem.* **105**, 971–981 (2008).
15. Malicdan, M.C., Noguchi, S., Nonaka, I., Hayashi, Y.K. & Nishino, I. A *Gne* knockout mouse expressing human GNE D176V mutation develops features similar to distal myopathy with rimmed vacuoles or hereditary inclusion body myopathy. *Hum. Mol. Genet.* **16**, 2669–2682 (2007).
16. Malicdan, M.C., Noguchi, S., Hayashi, Y.K. & Nishino, I. Muscle weakness correlates with muscle atrophy and precedes the development of inclusion body or rimmed vacuoles in the mouse model of DMRV/hIBM. *Physiol. Genomics* **35**, 106–115 (2008).
17. Comb, D.G. & Roseman, S. Composition and enzymatic synthesis of N-acetylneuraminic (sialic) acid. *J. Am. Chem. Soc.* **80**, 497–499 (1958).
18. Thomas, G.H., Scoocca, J., Miller, C. & Reynolds, L.W. Accumulation of N-acetylneuraminic acid (sialic acid) in human fibroblasts cultured in the presence of N-mannosamine. *Biochim. Biophys. Acta* **846**, 37–43 (1985).
19. Galeano, B. *et al.* Mutation in the key enzyme of sialic acid biosynthesis causes severe glomerular proteinuria and is rescued by N-acetylmannosamine. *J. Clin. Invest.* **117**, 1585–1594 (2007).
20. Robitaille, G., Ng-Kwai-Hang, K.F. & Monardes, H.G. Association of κ -casein glycosylation with milk production and composition in holsteins. *J. Dairy Sci.* **74**, 3314–3317 (1991).
21. Clarke, B.A. *et al.* The E3 ligase MuRF1 degrades myosin heavy chain protein in dexamethasone-treated skeletal muscle. *Cell Metab.* **6**, 376–385 (2007).
22. Kabeya, Y. *et al.* LC3, GABARAP and GATE16 localize to autophagosomal membrane depending on form-II formation. *J. Cell Sci.* **117**, 2805–2812 (2004).
23. Mizushima, N. & Yoshimori, T. How to interpret LC3 immunoblotting. *Autophagy* **3**, 542–545 (2007).
24. Kumamoto, T. *et al.* Proteasomes in distal myopathy with rimmed vacuoles. *Intern. Med.* **37**, 746–752 (1998).
25. Corfield, A.P. & Schauer, R. Occurrence of sialic acids. in *Sialic Acids. Chemistry, Metabolism, and Function* (ed. Schauer, R.) 5–50 (Springer, Wien, New York, 1982).
26. Helenius, A. How N-linked oligosaccharides affect glycoprotein folding in the endoplasmic reticulum. *Mol. Biol. Cell* **5**, 253–265 (1994).
27. Iijima, R., Takahashi, H., Namme, R., Ikegami, S. & Yamazaki, M. Novel biological function of sialic acid (N-acetylneuraminic acid) as a hydrogen peroxide scavenger. *FEBS Lett.* **561**, 163–166 (2004).
28. Askanas, V. & Engel, W.K. Inclusion-body myositis: a myodegenerative conformational disorder associated with A β , protein misfolding, and proteasome inhibition. *Neurology* **66** (suppl 1), S39–S48 (2006).
29. Spuler, S. *et al.* Dysferlin-deficient muscular dystrophy features amyloidosis. *Ann. Neurol.* **63**, 323–328 (2008).

ONLINE METHODS

Mice. All mouse protocols were approved by the Ethical Review Committee on the Care and Use of Rodents in the National Institute of Neuroscience, National Center of Neurology and Psychiatry. Generation of *Gne*^{-/-}hGNED176V-Tg (DMRV-hIBM) mice has been previously described¹¹. For all experiments, we used data from littermate mice (*Gne*^{+/-}hGNED176V-Tg, or wild-type) for comparison with DMRV-hIBM mice. We housed all animals mice in a barrier-protected facility that strictly adhered to specific pathogen-free-grade maintenance, and we maintained them on a 12-h to 12-h light-to-dark cycle with unlimited access to food and water. On average, an adult mouse takes about 14 mg per kg body weight per day of sialic acid from food.

Reagents. We purchased ManNAc and NeuAc from Japan Food and Liquor Alliance. Sialyllactose was from Sigma.

Treatment protocol. For ManNAc treatment, we grouped the DMRV-hIBM mice into four groups, and we gave them either water (control treatment) ($n = 5$) or daily increasing doses of ManNAc (mg per kg body weight per day). The low dose was 20 mg ($n = 5$), the medium dose was 200 mg ($n = 4$) and the high dose was 2,000 mg ($n = 4$). We also treated an equal number of littermates ($n = 18$). We added ManNAc into the drinking water, and we computed the dose according to weight. We adjusted the concentration in drinking water every 4 d depending on the amount of water the mice could drink. We initiated treatment from 5 weeks of age and continued until the mice reached at least 55 weeks of age.

For low-dose therapy, we gave the DMRV-hIBM mice either 20 mg per kg body weight per day ManNAc ($n = 6$), NeuAc ($n = 5$), sialyllactose ($n = 7$) or placebo ($n = 10$). We also treated equal numbers of littermates for all experimental groups. We diluted the metabolites into the drinking water and adjusted the doses every 4 d, similarly to ManNAc treatment. We started treatment at 10–20 weeks of age and continued until the mice reached at least 55 weeks of age.

We collected blood from tail every month for creatine kinase measurement and toxicology tests. At the end of the experimental protocol, we measured the weight of the mice, anesthetized them and collected the gastrocnemius for analysis of contractile properties (see below). We then killed the mice and collected their other organs for analysis.

Analysis of motor performance and contractile properties of the muscle. We evaluated the motor performance and measured the contractile properties of the gastrocnemius and tibialis anterior muscles according to previous protocols^{16,30} (see **Supplementary Methods** online).

Morphological analysis. We prepared and stained muscle cryosections according to published protocols^{15,31}. We counted the number of rimmed vacuoles in six transverse 10 μm -thick cryosections (at least 100 μm apart) stained with H&E on whole gastrocnemius sections for each group of mice.

For morphometric analyses, we stained sarcolemma of gastrocnemius muscle cryosections (see **Supplementary Methods**) and obtained six randomly selected digital images to evaluate single-fiber CSA as previously reported¹⁶.

Immunohistochemical analysis. We performed immunohistochemical analysis as described previously¹⁵ (see **Supplementary Methods**).

Preparation of protein fractions for sialic acid measurement. We prepared crude membrane fractions as previously reported³² (see **Supplementary Methods**).

Sialic acid measurement. We measured sialic acid concentration in the plasma and other organs as previously reported^{15,33}. We employed the same

methodology in determining the kinetics of NeuAc. In the plasma, the sialic acid detected represented mostly sialic acid conjugates and was $\leq 1\%$ free sialic acid.

Amyloid quantification. For quantifying the amount of amyloid in myofibers, we fixed six 10 μm -thick cryosections (each section was 100 μm apart) from the gastrocnemius muscle in paraformaldehyde for 30 min, followed by postfixation in ice-cold methanol. We immunostained sections with antibody to amyloid (clone 6E10, Covance) in a 1 in 400 dilution according to published protocols¹⁵. We counted as positive only signals within the myofibers in the whole gastrocnemius section.

We prepared samples for ELISA according to published protocols with slight modifications³⁴. For western blotting to detect the c99 fragment of β -amyloid precursor protein with antibody to amyloid, we extracted protein by 2 \times sample buffer containing 9.6% SDS, 4 M urea, 16% sucrose and 700 mM 2-mercaptoethanol, heated at 56 $^{\circ}\text{C}$ for 10 min. We resolved proteins by 10% bis-Tris (hydroxymethyl) methane SDS-PAGE (Invitrogen) under reducing conditions, transferred them to a nitrocellulose membrane and probed with antibody to β -amyloid (clone 6E10). For ELISA, we used the same method for protein homogenization, but we extracted protein using equal volumes of 0.4% diethylamine and 100 mM NaCl. We centrifuged samples at 100,000g for 1 h at 4 $^{\circ}\text{C}$ and pH-neutralized the supernatant with 0.5 M Tris base pH 6.8. We then used the supernatant for ELISA of β -amyloid 1–42 (Wako) and β -amyloid 1–40 (IBL) after brief vortexing. We normalized the amount of amyloid per mg protein. For plasma amyloid, we used 50 μl of thawed plasma.

Biochemical and toxicology assays. We measured serum creatine kinase as previously described¹⁵. We determined the activity of plasma alkaline phosphatase using the Japanese Society of Clinical Chemistry method³⁵, with *p*-nitrophenylphosphate as substrate and ethylaminoethanol-HCl as buffer. We measured alanine transaminase by determining the reduction of NADH (Kyowa Medics). We assayed blood urea nitrogen by an automatic clinical analyzer (Dri-Chem 3,500 V, Fuji Film). We made all measurements three times.

Sialic acid and N-acetylmannosamine pharmacokinetics. See **Supplementary Methods** online.

Statistical analyses. All values are expressed as means \pm s.e.m., except for single-fiber diameter, for which values are expressed as mean \pm range. For survival analysis, we used the Kaplan-Meier method to draw the survival curve and used the log-rank test and the Gehan-Breslow-Wilcoxon test to compare groups. For other analysis to determine significance among groups, we used one-way analysis of variance with Dunnett's post-test to compare the treatment group with the placebo group. For the computation of odds ratio, we used Fisher's exact test. We set the level of significance to $P < 0.05$ for all analyses.

- Lynch, G.S., Hinkle, R.T., Chamberlain, J.S., Brooks, S.V. & Faulkner, J. Force and power output of fast and slow skeletal muscles from mdx mice 6–28 months old. *J. Physiol. (Lond.)* **535**, 591–600 (2001).
- Malicdan, M.C., Noguchi, S. & Nishino, I. Monitoring autophagy in muscle diseases. *Methods Enzymol.* **453**, 379–396 (2009).
- Gagiannis, D., Gossrau, R., Reutter, W., Zimmermann-Kordmann, M. & Horstkorte, R. Engineering the sialic acid in organs of mice using *N*-propanoylmannosamine. *Biochim. Biophys. Acta* **1770**, 297–306 (2007).
- Hara, S. *et al.* Determination of mono-*O*-acetylated *N*-acetylneuraminic acids in human and rat sera by fluorometric high-performance liquid chromatography. *Anal. Biochem.* **179**, 162–166 (1989).
- Schmidt, S., Jiang, Y., Nixon, R. & Mathews, P. Amyloid proteins methods and protocol. in *Methods in Molecular Biology* Vol. 299 (ed. Sigurdsson, E.M.) 408 (Humana Press, New York, 2004).
- Kotani, K., Maekawa, M. & Kanno, T. Reestimation of aspartate aminotransferase (AST)/alanine aminotransferase (ALT) ratio based on JSCC consensus method—changes of criteria for a differential diagnosis of hepatic disorders following the alteration from Karmen method to JSCC method [in Japanese]. *Nippon Shokakibyo Gakkai Zasshi* **91**, 154–161 (1994).